Synthesis and Characterization of Nano-Sized NiO and Its Surface Catalytic Effect on Poly(vinyl alcohol)

S. Gandhi,[1] N. Nagalakshmi,[2] I. Baskaran,[2] V. Dhanalakshmi,[1] M. R. Gopinathan Nair,[3] R. Anbarasan[4]

[1]*Department of Polymer Technology, Kamaraj College of Engineering and Technology, Virdhunagar 626 001, Tamilnadu, India*
[2]*Department of Chemistry, Saraswathy Narayanan College, Madurai 625 022, Tamilnadu, India*
[3]*School of Chemical Sciences, Mahatma Gandhi University, Kottayam 686 560, Kerala, India*
[4]*Department of Mechanical Engineering, MEMS Thermal Control Lab, National Taiwan University, Taipei 10617, Taiwan, Republic of China*

Received 25 August 2009; accepted 7 April 2010
DOI 10.1002/app.32570
Published online 3 June 2010 in Wiley InterScience (www.interscience.wiley.com).

ABSTRACT: Nickel oxide (NiO) nano particle is synthesized by Ultrasound assisted one pot method and thus synthesized nano NiO is mixed with poly(vinyl alcohol) (PVA) to prepare the PVA/NiO nanocomposite. The influence of the composition on the structural modification on the composite is evaluated. The particle size and morphology of NiO nano material is confirmed by HRTEM. The structure and properties of the PVA/NiO nanocomposite material are characterized by FTIR, XRD, UV–Visible spectroscopy, DSC, TGA, and HRTEM. The synthesized PVA nanocomposite underwent hydrolytic oxidation reaction assisted by the effect of nano-sized NiO. © 2010 Wiley Periodicals, Inc. J Appl Polym Sci 118: 1666–1674, 2010

Key words: nano NiO; PVA; characterizations; HRTEM; nano composite

INTRODUCTION

In recent years there has been an increasing interest in the synthesis of nano-sized metal oxides because of their large surface area, unusual adsorptive properties, surface defects, and fast diffusivities[1] and the nano materials have extensively attracted interests for their small and quantum-size effects. Nano materials can exhibit novel and significant mechanical, electronic, magnetic, and optical properties in comparison with their bulk counterparts.[2] Nickel oxide (NiO) is a very important material extensively used in catalysis, battery cathodes, gas sensors, electrochromic films, and magnetic materials.[3,4] NiO catalyst exhibits good low temperature catalytic performance for oxidative dehydrogenation of ethane (ODHE) to ethylene reaction.[5] There are many methods available on the preparation of NiO nano particles, such as precipitation method, micro-emulsion method, solid-state method, etc.[6,7] However, to some extent, these preparation methods have some disadvantages. The precipitation method is affected by the factors like precipitation agent, pH, and temperature and solution concentration; hence the process is difficult to control. The micro-emulsion and solid-state methods are not mature in technology. Amongst the several investigated methods, the ultra sound (US) assisted one pot method to prepare ultrafine particles represented an effective pathway. In sono-chemical method, ultrasonic waves have been used extensively to generate novel materials with unusual properties, because it can induce the formation of particles with much smaller size and higher surface area than those reported by other methods. The chemical effects of ultrasound arise from acoustic cavitations, i.e., the formation, growth, and implosive collapse of bubbles in liquid which generates transient temperature of ~5000 K, pressure of ~1800 atmosphere and cooling rate in excess of 1010 K/s.[8] These extreme conditions can drive chemical reactions, such as oxidation, reduction, dissolution, and decomposition, which have been explored to generate metal carbides and metal oxides.[9,10] Xie et al.[11] synthesized NiO and NiO/TiO_2 nano composites through ultrasonication method for supercapacitor applications. US assisted synthesis of NiO for memory application is reported in the literature.[12] The bare or surface modified NiO particles find application in areas, such as hyperthermia treatment of cancer and magnetic field assisted radioactive chemical separation.[13] Particularly, the usage of inorganic–organic composite materials is becoming increasingly important due to their extraordinary properties, which arises from the

Correspondence to: R. Anbarasan (anbu_may3@yahoo.co.in).

synergism between the properties of the individual components and their interactions with the base matrix materials. Several ways of incorporating inorganic materials into organic polymers have been attempted in the earlier literature.[14,15] Among the many polymers used, poly(vinyl alcohol) (PVA) has been recently used to develop inorganic–organic nanocomposite hybrids.[16] PVA is known to be one of the most widely used membranes for the separation of water-organic mixtures in addition to its use as adhesives coatings and paints in view of its good film-forming nature, hydrophilicity, processability, and good chemical resistivity.[17] Physical properties of PVA doped with some transition metal salts have been investigated.[18] Recently, Vijayakumar et al.[19,20] had successfully prepared various nano-sized metal oxides and metal oxide-polymer nanocomposite materials. By thorough literature survey, we could not find any report based on PVA/NiO nano composite with FTIR based kinetic study. In this investigation, for the first time, we have reported about the synthesis of PVA/NiO nano composite systems and further characterized with FTIR, XRD, UV–Visible spectroscopy, differential scanning calorimetry (DSC), thermogravimetric analysis (TGA) and High-resolution transmission electron microscopy (HRTEM) like analytical tools to study the structure-property relationship. The NiO based polymer nano composites are found applications in battery field and solid-oxide fuel cell field.[21–23] The aim of this investigation is to synthesize the nano-sized NiO through US assisting, and the effect of the same on the structure-property relationship of PVA, particularly with the thermolytic and hydrolytic oxidation reactions through FTIR-RI method.

EXPERIMENTAL

Materials

Nickel acetate and Hydrochloric acid were purchased from Ottochemi, India. Poly(vinyl alcohol) (PVA, S.D. Fine Chemicals, India, 12.5 kDa – weight average molecular weight with 85% hydrolyzed) was used without further purification. Brydson Ultrasonicator, with the frequency of 40 kHz was used for ultrasound generation purpose. Doubly distilled (DD) water was used for the preparation of reactant solutions.

Synthesis of nano-sized NiO

Nanostructure NiO was synthesized by the one pot sonochemical method. In a typical experimental procedure: 5 g of nickel acetate monohydrate was dissolved in 100 mL of deionized water in a beaker, which was placed in an ice bath, and 10 mL of concentrated HCl was poured drop wise in this solution while stirring it continuously. The stirring was continued for 10 min. Subsequently, the resultant solution was first sonicated at 40 kHz for 30 min in ice bath, then, at room temperature while the solution temperature was raised to 80°C and heated the solution to 130°C with simultaneous ultrasonication.[24] The precipitate was filtered and washed with the methanol several times to remove ionic impurities and finally dried under vacuum for 48 h at room temperature. The chemical purity and water content of thus synthesized NiO was analyzed through FTIR spectroscopy and further supported by DSC and TGA techniques. The size distribution of NiO was checked through recording HRTEM topography. The surface catalytic effect of NiO was investigated through FTIR-RI method. The surface area of NiO by nitrogen adsorption isotherm experiment is going on in our lab.

Preparation of PVA/NiO nanocomposite film

PVA was used as basic polymeric material in this work. PVA films were prepared by using a casting technique.[25] Casting technique is suitable for preparing films without pores and voids. Moreover, this method produced a film with uniform thickness. Hence we preferred the casting technique. PVA solution was prepared by dissolving 1.0 g PVA in DD water and maintained for 24 h at room temperature to swell. The solution was then warmed up to 60°C and thoroughly stirred using a magnetic stirrer for 4 h until the polymer dissolved in water medium completely. Then, 2% weight of NiO was added and stirred well for further 24 h. The solution was poured onto polyimide film to get a film with uniform thickness. Homogeneous films were obtained after drying in an air oven for 48 h at 40°C and PVA films filled with as synthesized nano-sized NiO mass fractions of 4, 6, 8, and 10% were prepared using the same method. The prepared films were free from air bubbles and with uniformly dispersed NiO particles on PVA matrix. The thicknesses of the produced films were in the range of 0.1–0.21 mm and cut into pieces suitable for measurements. The film samples are convenient for further processing and hence we preferred the casting film formation method.

Characterizations

The FTIR spectrum was recorded using a SHIMADZU FTIR-8400 S model instrument. UV–Visible absorption spectra were measured by using Perkin Elmer UV–Visible instrument. XRD of the samples were recorded with a help of Philips PW 1050/80 diffractometer with Ni-filtered CuKα radiation

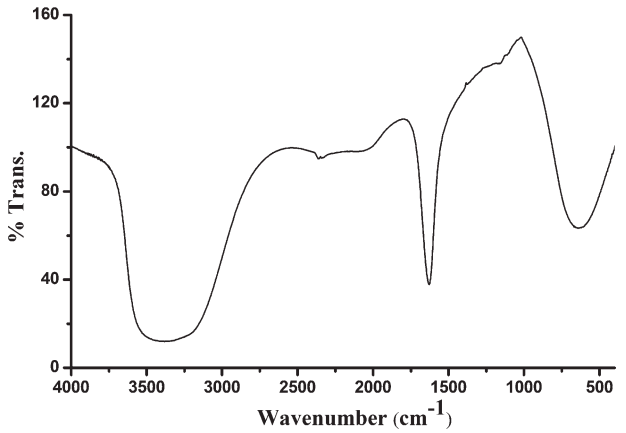

Figure 1 FTIR spectrum of nanosized NiO.

generated with the settings of 30 kV and 15 mA. Thermal analyses were performed by DSC using SHIMADZU DSC-50 under nitrogen atmosphere at the heating rate of 10°C/min. The thermal stability of nanocomposite was examined by TGA instrument by using STA 1500 PL Thermal Sciences instrument under air atmosphere at the heating rate of 10°C/min from room temperature to 500°C. Synthesized nano material topography and size were observed by HRTEM on a JEM-200 CX transmission electron microscope. From the FTIR spectrum, the corrected peak area of the peaks was determined after proper baseline correction by using FTIR software. The relative intensity (RI) of the peaks was determined as follows:

$$\text{RI of C=O} = \text{RI}_{[\text{C=O/CH}]} = A_{1733}/A_{844} \quad (1)$$

$$\text{RI of C=C} = \text{RI}_{[\text{C=C/CH}]} = A_{1661}/A_{844} \quad (2)$$

RESULTS AND DISCUSSION

For the sake of convenience the results and discussion part is sub-divided into two parts namely, (1) synthesis and characterizations of nano-sized NiO and (2) synthesis and characterizations of PVA/NiO nano composites.

Synthesis and characterization of nano-sized NiO

Infrared spectroscopy

The FTIR spectrum of pristine NiO is given in Figure 1. The important peaks of NiO are discussed here. The metal-oxygen (M—O) bond was observed at 650 cm^{-1}. A broad band in the range of 3600–3100 cm^{-1} is due to the OH stretching of water molecules associated with NiO. A peak between 1670 and 1600 cm^{-1} is corresponding to the OH bending vibration of water molecules. Recently, Anbarasan and research team[26] explained the M—O stretching in $Ni(OH)_2$. This investigation is in accordance with their report. In this investigation we are mainly focusing on the M—O stretching, because the aim of this investigation is the synthesis of NiO. By identifying the M—O stretching in the FTIR spectrum at 650 cm^{-1} the structure of NiO is confirmed.

X-ray diffraction analysis

Figure 2 displays the X-ray diffraction pattern of pristine NiO. It can be seen three distinct diffraction peaks at the 2θ value of 37, 43, and 63° for the nano-sized NiO. These peaks are corresponding to the (1 1 1), (2 0 0), and (2 2 0) crystal planes of cubic NiO.[27] A peak at 16.1° is responsible for crystalline nature and increase in basal spacing of NiO nano crystals. The synthesized NiO nano particles are semicrystalline in nature and which can be confirmed from the broadening the diffraction peak with weaker intensity.

High-resolution transmission electron microscopy analysis

HRTEM images of the NiO nano particle is depicted in Figure 3. Figure 3(a) indicates the layered structure of NiO with the length of 20–25 nm and has the breadth of <1 nm. Figure 3(b) represents the dispersion of agglomerated stacks of nano-sized NiO. During the synthesis of nano-sized NiO, we found some agglomerated form of NiO with the size of 0.2 to 0.3 μm [Fig. 3(c)]. Generally, the agglomerated form will show a lower surface catalytic effect than the nano sized particle. The SAED [Fig. 3(d)] indicates the semicrystalline nature of pristine NiO. The HRTEM report concluded that even though ultrasound was used for the dispersion of agglomerated nano material during the synthesis, some agglomerated form of NiO was also formed and which was an unavoidable one. This urged us to find out the role of

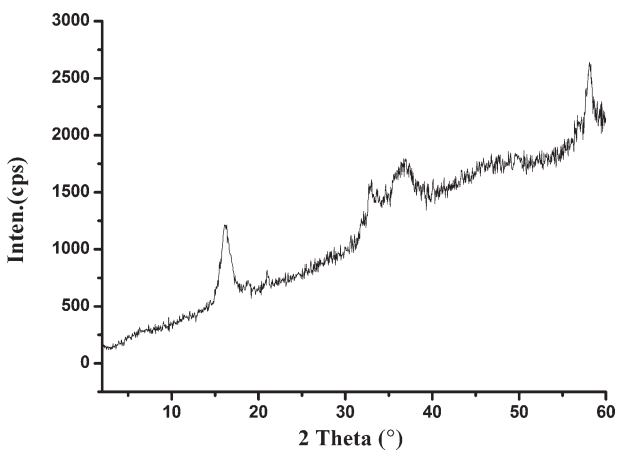

Figure 2 XRD spectrum of nanosized NiO.

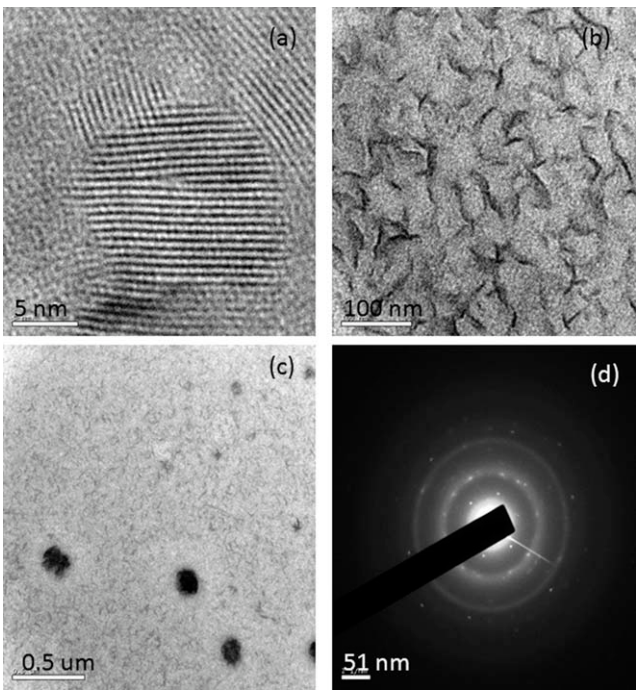

Figure 3 HRTEM image of NiO nanoparticle.

dispersant like aniline during the nano particle synthesis. But, in this investigation the role of dispersing agent is not included for the sake of convenience.

Synthesis and characterizations of PVA-NiO nano composites

Infrared spectroscopy

The FTIR spectra of pristine PVA and PVA filled with various mass fractions of NiO is exhibited in Figure 4. Figure 4(a) confirms the FTIR spectrum of pristine PVA. The important peaks of PVA are characterized below. A strong broad band at 3425 cm^{-1} is assigned to O—H stretching vibration of hydroxyl groups of PVA. The band corresponding to C—H asymmetric stretching vibration occurred at 2928 and C—H symmetric stretching vibration at 2853 cm^{-1}. A band at 1733 cm^{-1} corresponds to the C=O stretching vibration (of vinyl acetate group of PVA) and 1640 cm^{-1} corresponds to a C=C group in PVA backbone. The sharp band at 1089 cm^{-1} is responsible for the C—O—C stretching of ester group present in the PVA backbone. The corresponding bending and wagging of CH_2 vibrations are observed at 1438 and 1378 cm^{-1} respectively, and C—H wagging at 1247 cm^{-1}.[28,29]

The incorporation nano-sized NiO in PVA caused the slight changes in the intensities of absorption bands at 1733 and 1640 cm^{-1} and the formation of new absorption bands in the range of 1000–600 cm^{-1}. Peak around 1000–600 cm^{-1} is attributed to the metal-oxygen stretching of NiO.[30] This confirmed the presence of nano-sized NiO particles present in PVA matrix. The intensities of peaks at 1733 and 1640 cm^{-1} assigned to C=O stretching and C=C group in PVA backbone were increased while increasing the composition of nano NiO. The added nano NiO was simply acting as a catalyst for the oxidation process in the PVA backbone, which was confirmed in the FTIR spectroscopy analysis. The added nano-sized NiO altered the structure of PVA in two ways. First, it activated the conversion of secondary alcoholic group into a keto group via thermolytic oxidation reaction. Secondly, it boosted the formation of C=C double bonds along the PVA chains through its surface catalytic effect. The C=C double bond may be formed at the PVA chain end or in the middle of PVA chain. During this nano composite preparation in aqueous medium at higher temperature led to the intercalation of PVA chains into the basal spacing of NiO, which can be confirmed by the HRTEM analysis. The order of structural changes in PVA backbone due to the nano NiO was measured by plotting the relative intensities of carbonyl and relative intensities of alkenes in PVA and weight percentage of nano NiO. It is shown in Figure 5. It was observed that the added nano NiO converted the secondary alcoholic group into keto and oxidized the vinyl group into alkenes in the PVA backbone. The plot of log (% weight of NiO) vs. log ($RI_{[C=O/CH]}$) [Fig. 5(a)] and log (% weight of NiO) vs. log ($RI_{[C=C/CH]}$) [Fig. 5(b)] indicate a straight line with the slope value of 0.99 and 0.48. These slope values confirmed the 1.0 order of ketone formation and 0.5 order of alkene formation reaction with respect to (% weight of NiO). In our earlier communication, also we observed this type of observations

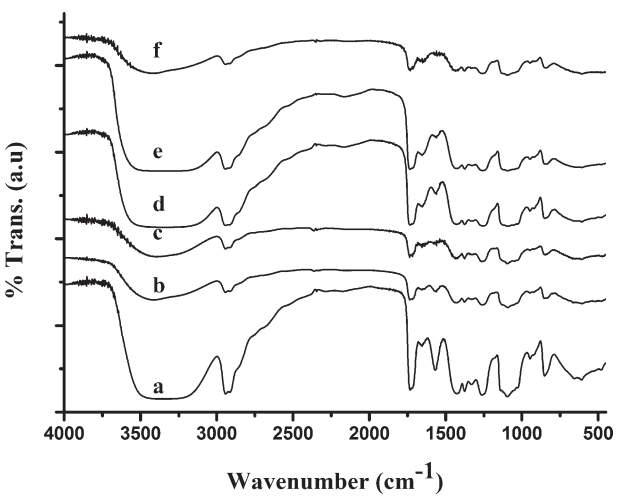

Figure 4 FTIR spectra of PVA loaded with NiO at (a) 0% weight, (b) 2% weight, (c) 4% weight, (d) 6% weight, (e) 8% weight, (f) 10% weight.

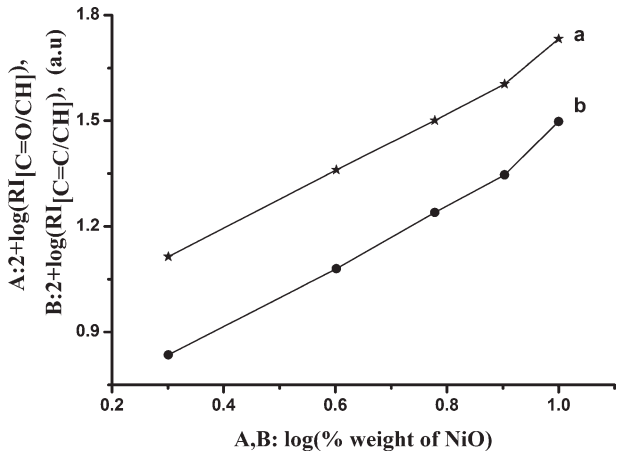

Figure 5 Effect of (% weight of NiO) on (a)$RI_{[C=O/CH]}$, (b)$RI_{[C=C/CH]}$ of PVA.

during the nano composite preparation between PVA and metal hydroxides.[31]

X-ray diffraction analysis

Figure 6 reveals the XRD scans of pristine PVA and PVA containing different % weight loading of NiO. It is obvious that there is no significant effect on the general shape of the XRD pattern. The observed spectra characterized a semi crystalline polymer possessing a clear crystalline peak for all studied samples. This corresponds to a (101) crystal plane with the *d* spacing of 4.57 A° for PVA[32] which indicates the semi crystalline nature of PVA. The crystalline nature of PVA results from the strong intermolecular interaction between PVA chains through intermolecular hydrogen bonding. The intensity of the diffraction peak and the size of the crystals in PVA are determined by the number of PVA chains packed together. The intensity of the PVA main diffraction peak (101) is further decreased due to the host effect of nano NiO. This is because of interactions between PVA and mixed NiO lead to a decrease in the intermolecular interaction between PVA chains and thus the lower crystalline degree.[18]

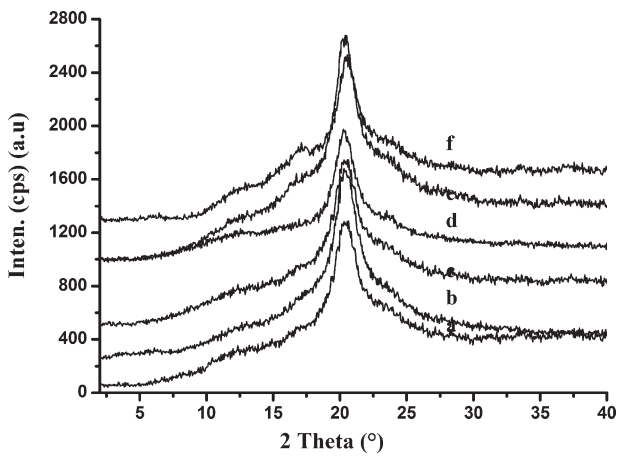

Figure 6 XRD of PVA loaded with NiO at (a) 0% weight, (b) 2% weight, (c) 4% weight, (d) 6% weight, (e) 8% weight, (f) 10% weight.

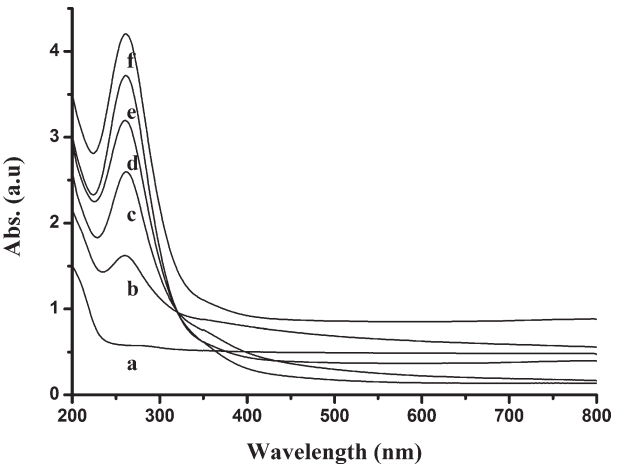

Figure 7 UV-Visible spectra of PVA loaded with NiO at (a) 0% weight, (b) 2% weight, (c) 4% weight, (d) 6% weight, (e) 8% weight, (f) 10% weight.

UV–Visible spectra

The UV–Visible spectra of pristine PVA and PVA/NiO nanocomposites are shown in Figure 7. The pristine PVA did not show any peak in the UV–Visible spectrum [Fig. 7(a)]. Most commercial PVA absorbs strongly in the 200–400 nm region due to the presence of unhydrolyzed acetate group in PVA backbone.[18] The spectrum of the NiO loaded PVA samples contain an absorption peak at 280 nm and a shoulder at about 265 nm [Fig. 7(b–f)]. These bands are attributed to carbonyl-containing segments of the general form $O(CH{=}CH)_n$ CO—, where *n* 1,2,..., resulting from hydrolytic and thermolytic oxidation reactions. The shoulder at 265 nm is due to the absorption by simple carbonyl groups along the polymer chain. The peak at 280 nm is assigned to the carbonyl groups associated with ethylene unsaturation of the type $O(CH{=}CH)_2$ CO—, and is indicative of the presence of double bonds on PVA backbone.

There was no additional peak and observable changes in the band position with all loading levels of 2, 4, 6, 8, and 10% weight of NiO. It revealed that there was no strong complex formation between the Ni^{2+} ion with the hydroxyl group of PVA. It is consistent with Lee and coworkers[33] report for PVA–ZnO nanocomposite system and also they reported that the intensity of the absorption peaks increased with increasing the NiO loading level. The dependence of the intensity of the bands on the NiO loading level provided an evidence for the surface

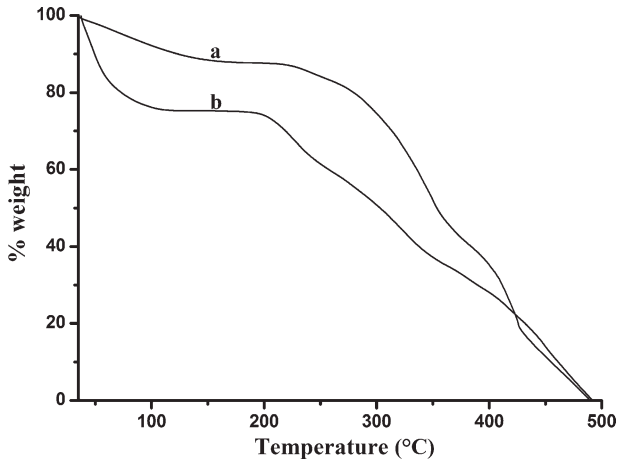

Figure 8 TGA of PVA in (a) powder form, (b) film form.

catalytic effect of nano-sized NiO on the PVA backbone, i.e., the added nano-sized NiO activated the oxidation and thermal degradation processes in aqueous condition during the polymer-nano composite preparation. Hence, while increasing the % weight loading of nano-sized NiO; the simultaneous oxidation effects are also increased. As a result, there will be a formation of more and more ketone and alkene groups. These two effects combined with each other and appeared as a sharp peak around 280 nm.

Thermogravmetric analysis

Thermal stability of the polymer nanocomposites was evaluated by TGA. The thermogravimetric graph of pristine PVA powder and pristine PVA film are represented in Figure 8. Figure 8(a) indicates the TGA of PVA in powder form with three step degradation process. The first minor weight loss step up to 130°C is responsible for the removal of moisture and physisorbed water molecules. The second major weight loss step above 200°C is associated with the dissociation of intermolecular and intramolecular hydrogen bonding with PVA chain degradation. The third minor weight loss step around 378°C is due to the degradation of acetate group of PVA (PVA is 85% hydrolyzed). The TGA thermogram of PVA in film form is given in Figure 8(b) with two step degradation process. The first minor weight loss around 113°C is accounted by the removal of moisture and physisorbed water molecules. The presence of physisorbed water molecules on the PVA backbone is further supported with the DSC heating scan of PVA/NiO nano composite system in the forthcoming session. The second major weight loss step above 200°C is explained on the basis of breaking of inter and intra molecular hydrogen bonding with simultaneous degradation of PVA chain. Here the third minor weight loss due to the degradation of acetate group is not observed due to the possible hydrolysis in an aqueous medium. The PVA was dissolved in water molecules at 85°C and then made into a thin film. During this film preparation, the acetate groups were possibly hydrolyzed. In comparison, the PVA in film form exhibited lower thermal stability due to the presence of larger amount of physisorbed water molecules. Rachna and Rao[34] reported about the thermal degradation of PVA. Our reports are coinside with them.

The TGA of PVA loaded with NiO at different % weight is given in Figure 9(a–e) with two step degradation process. As usual, the first minor weight loss step below 100°C is due to the removal of moisture and loosely bounded water molecules from PVA chain. The second major weight loss step around 215°C is explained by the PVA chain degradation step. In comparison, the initial degradation temperature (T_{id}) of PVA/NiO nano composite is greater than that of PVA in both powder and film forms. Moreover, the % weight residue remains above 350°C is increased with simultaneous increase of % weight loading of NiO. These two major points are discussed below. (1) During the preparation of PVA/NiO nano composite, there is a chance for the formation of intercalation of PVA chains into the basal spacing of NiO. Because of the umbrella effect, the thermal stability of PVA was increased with the increase of % content of NiO. (2) During the preparation of PVA/NiO nano composite, there is a chance for the formation of exfoliated NiO platelets and distribution of the same uniformly on the PVA matrix. Thus formed NiO platelets protect the PVA chains from the thermal force. By the way of intercalation and exfoliation, the thermal stability of PVA was activated. Approximately 50% weight is remained above 350°C at 10% weight of NiO loading on PVA backbone. The introduction of NiO

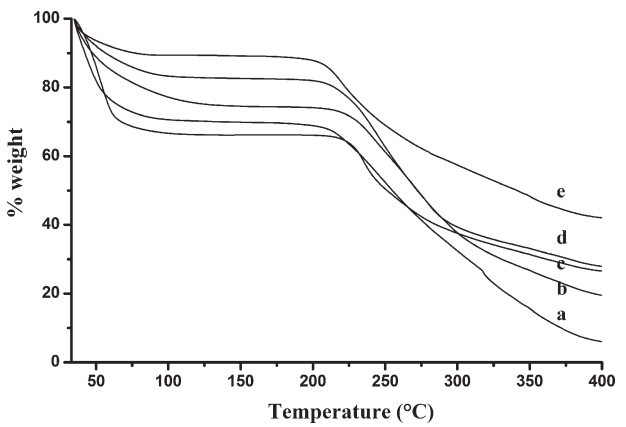

Figure 9 TGA of PVA loaded with NiO at (a) 2% weight, (b) 4% weight, (c) 6% weight, (d) 8% weight, (e) 10% weight.

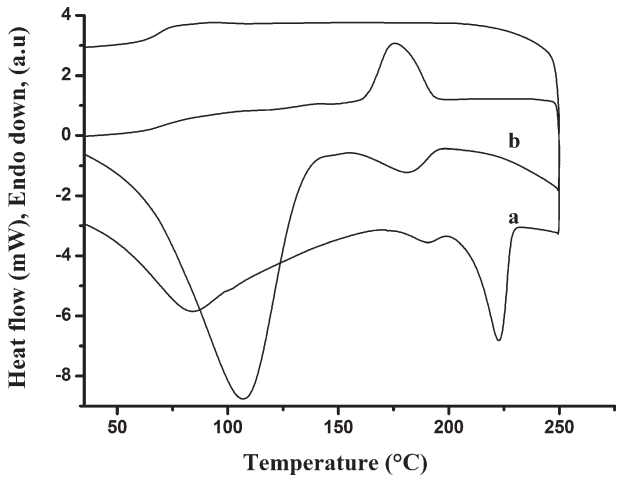

Figure 10 DSC of PVA in (a) powder form, (b) film form.

nanoparticles in PVA matrix greatly improved the thermal resistance. Therefore, the PVA/NiO nanocomposite is thermally more stable than the pristine PVA. Zheng and Ling[35] reported the similar result for filled SiO_2–PVA nanocomposite system.

Differential scanning calorimetry

DSC in the temperature ranged from room temperature to 250°C (Fig. 10) studied the thermal behavior of pristine PVA in the form of powder and film. Figure 10(a) exhibits the DSC scan of PVA in powder form. The DSC scan showed three endo thermic peaks corresponding to de-watering temperature ($T_{d.w}$) (83.5°C), alpha transition temperature (T_α) (190.6°C) and melting temperature (T_m) (222.4°C) with one exo thermic peak corresponding to crystallization temperature (T_c) (175.1°C). The DSC scan of PVA film [Fig. 10(b)] exhibited two endo thermic peaks at 106.5 and 181.3°C with respect to $T_{d.w}$ and T_α. In this system, the T_m and T_c were absent. This confirmed the amorphous nature of the PVA film. PVA is a crystalline bio-degradable polymer with a stable α-crystalline (inner micro structure) form. When PVA is heated up to its T_m, the α-form is more and more clear and stable. Beyond certain temperature the stable α-form is converted into other forms like β or γ with lower thermal stability.

The DSC heating scan of various % weight of NiO loaded PVA is shown in Figure 11(a–e). The DSC heating scan showed one broad endo thermic peak around 90°C corresponding to $T_{d.w}$. The important point noted here is while increasing the % weight loading of NiO onto PVA backbone, the $T_{d.w}$ is shifted towards lower temperature. The $T_{d.w}$ of PVA at 2 and 10% weight loading of NiO is 95.8 and 82.1°C respectively. This indicated that while increasing the % weight of NiO, the amount of physisorbed water molecules by PVA was drastically reduced i.e., the hydrophobicity is increased with the increase of NiO content, due to its nano size.[36,37] The decrease in water content with the increase of NiO content was already supported by the TGA of PVA/NiO systems [Fig. 9(a–e)]. Moreover, due to the hydrolytic and thermolytic oxidation reactions, the crystallinity of PVA chain was decreased. The FTIR-RI confirmed the decrease in crystallinity of PVA through the formation of ketone and olefin groups. This is in accordance with our earlier communications.[36–38]

High-resolution transmission electron microscopy

Figure 12 shows the HRTEM images of the 10% weight nano NiO loaded PVA matrix. Figure 12(a) indicates the intercalation of PVA chain into the basal spacing of layered NiO. The agglomerated NiO nano particles combined with each other and formed different shapes like sphere, triangle, and hexagon [Fig. 12(b)]. The agglomerated shapes are having the size of 100 nm. The sphere are having the lowest size of <50 nm [Fig. 12(c)] and the SAED indicates [Fig. 12(d)] the improved amorphous character of PVA/NiO nano composite system due to heavy loading of semi crystalline NiO. This proved that after making nano composite with 10% weight of NiO, the total system became an amorphous one due to heavy loading.

CONCLUSIONS

From the above study the important points are presented here as conclusions. (1) Nano-sized NiO were synthesized by one pot sono-chemical method for the surface catalytic effect. (2) FTIR spectrum confirmed the presence of metal-oxide stretching in the

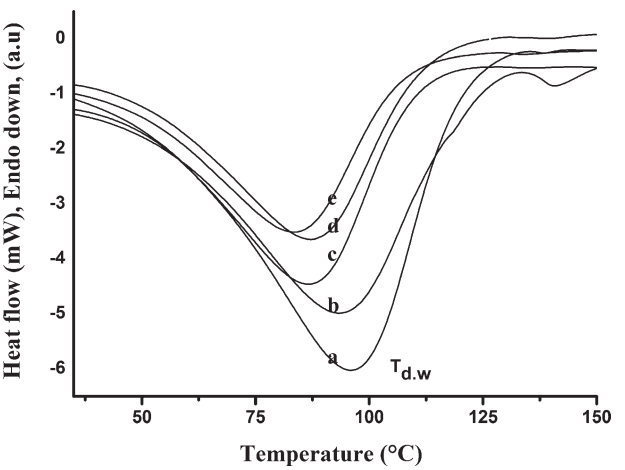

Figure 11 DSC of PVA loaded with NiO at (a) 0% weight, (b) 2% weight, (c) 4% weight, (d) 6% weight, (e) 8% weight, (f) 10% weight.

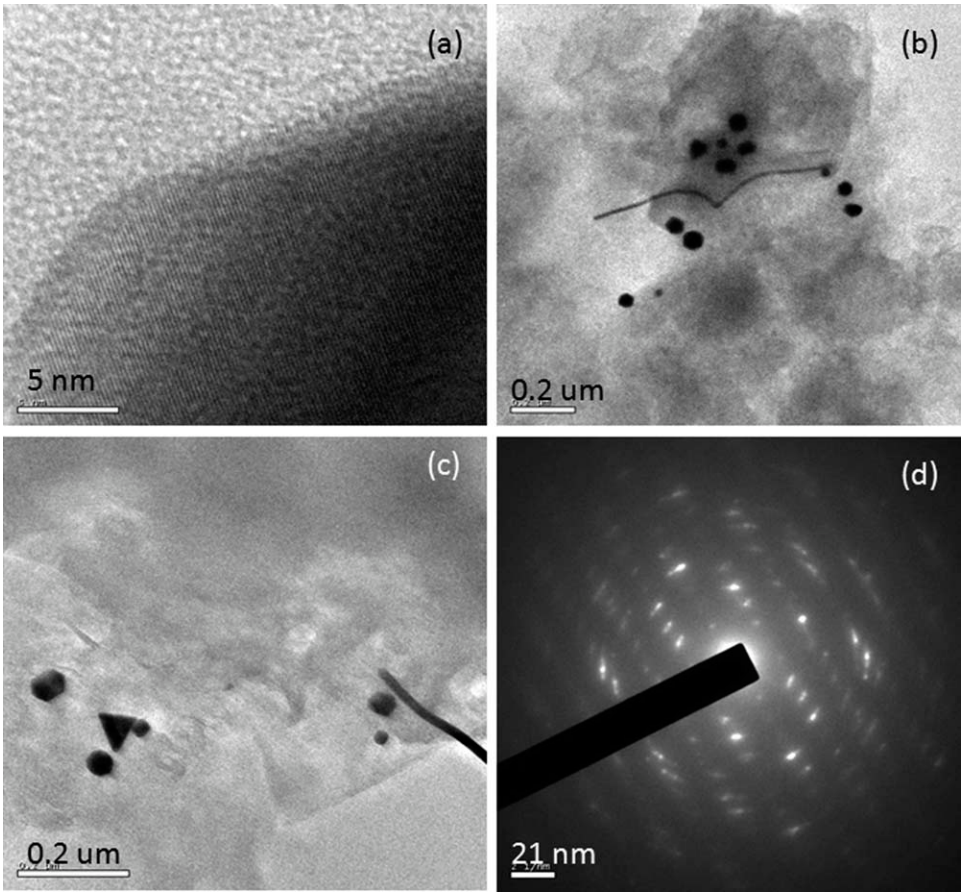

Figure 12 HRTEM topography of PVA-10% weight NiO nanocomposite system.

nano-sized NiO at 650 cm^{-1}. (3) XRD spectral study suggested a semi crystalline nature of nano-sized NiO. (4) HRTEM image of the NiO nano particles confirmed the size about 50–60 nm length with <1 nm breadth. (5) The structure of PVA was altered during the incremental loading of nano-sized NiO. (6) Because of the surface catalytic effect of nano-sized NiO on the PVA backbone, the secondary alcoholic groups were converted into ketone and C=C groups. (7) The FTIR-RI study indicated the 1.0 order ketone formation and 0.50 order olefin formation reactions during the incremental loading of NiO which confirmed the surface catalytic activity of nano-sized NiO. (8) DSC inferred that the PVA film and PVA/NiO nano composite systems became amorphous due to thermolytic and hydrolytic oxidation reactions. (9) TGA exhibited the increased in char forming behavior of PVA after loading with different % weight of NiO. (10) The HRTEM topography of PVA/10% weight NiO nano composite system showed the agglomerated nano sphere, hexagon, and triangle like morphology. (11) The overall conclusion from this investigation is the nano-sized NiO altered the structure of PVA in an aqueous medium due to the thermolytic and hydrolytic oxidation reactions and in such a way the nano-sized NiO exhibited its surface catalytic effect on the PVA backbone.

References

1. Adair, J. H.; Li, T.; Kido, T.; Havey, K.; Moon, J.; Mecholsky, J.; Morrone, A.; Talham, D. R.; Ludwig, M. H.; Wang, L. Mater Sci Eng Rep 1998, 23, 139.
2. Bargava, R. N. J Lumin 1996, 70, 85.
3. Yoshio, M.; Todorov, Y.; Yamato, K.; Noguchi, H.; Itoh, J.; Okada, M.; Mouri, T. J Power Sources 1998, 74, 46.
4. Alcantara, R.; Lavela, P.; Tirado, J. L.; Stoyanova, R.; Zhecheva, E. J Electrochem Soc 1998, 145, 730.
5. Wu, Y.; Chen, T.; Weng, W. Z.; Wan, H. L. Chin J Catal 2003, 24, 403.
6. Han, D. Y.; Yang, H. Y.; Shen, C. B. Powder Technol 2004, 147, 113.
7. Wang, Y. P.; Zhu, J. W.; Yang, X. J. Thermochim Acta 2005, 437, 106.
8. Suslick, K. S.; Cichowlas, A. A.; Grinstaff, M. W. Nature 1991, 353, 414.
9. Okitsu, K.; Mizukoshi, Y.; Bandow, H.; Maedu, Y.; Yamamoto, T.; Nagata, Y. Ultrason Sonochem 1996, 3, S249.
10. Hyeon, T.; Fang, M.; Suslick, K. S. J Am Chem Soc 1996, 118, 5492.
11. Xie, Y.; Huang, C.; Zhou, L.; Huang, H. Compos Sci Technol 2009, 69, 2108.
12. Park, J. W.; Kim, D. Y.; Lee, J. K. J Vac Sci Technol 2005, 23, 1309.
13. Bahadur, D.; Giri, J.; Nayak, B. B. Pramana J Phys 2005, 65, 663.

14. Judeinstein, P.; Sanchez, C. J Mater Chem 1996, 6, 511.
15. Schubert, U.; Husing, N. Synthesis of Inorganic Materials; Wiley-VCH: New York, Weinheim, 2000.
16. Kickelbick, G. Prog Polym Sci 2003, 28, 83.
17. Krumova, M.; Lopez, D.; Benavente, R.; Mijangos, C.; Perena, J. M. Polymer 2000, 41, 9265.
18. Zidan, H. M. Polym Test 1999, 18, 449.
19. Vijayakumar, R.; Diamant, Y.; Gedanken, A. Chem Mater 2000, 12, 2301.
20. Vijayakumar, R.; Elgamiel, R.; Diamant, Y.; Norwig, J.; Gedanken, A. Langmuir 2001, 17, 1406.
21. Liu, J.; Madsen, B. D.; Ji, Z.; Barnet, S. A. Electrochem Solid State Lett 2002, 5, A122.
22. Wu, M. S.; Wang, M. J. Electrochem Solid State Lett 2010, 13, A1.
23. Smitha, B.; Sridhar, S.; Khan, A. A. J Memb Sci 2005, 259, 10.
24. Yang, L.-X.; Zhu, Y.-J.; Tong, H.; Wang, W.-W. Ultrason Sonochem 2007, 14, 259.
25. Zidan, H. M. J Appl Polym Sci 2003, 88, 516.
26. Fathima Parveen, M.; Umapathy, S.; Dhanalakshmi, V.; Anbarasan, R. NANO 2009, 4, 1.
27. Ying, W.; Yiming, H.; Tinghua, W.; Weizheng, W.; Huilin, W. Mater Lett 2007, 61, 2679.
28. Soliman Selim, M.; Seoudi, R.; Shabaka., A. A. Mater Lett 2005, 59, 2650.
29. Shin, E. J.; Lee, Y. H.; Choi, S. C. J Appl Polym Sci 2004, 91, 2407.
30. Abdelaziz, M.; Abdelrazek., E. M. Phys B 2007, 390, 1.
31. El-Tantawy, F.; Abdelkader, K. M.; Kane Ko, F.; Sung, Y. K. Eur Polym J 2004, 40, 415.
32. Yu, Y. H.; Lin, C. Y.; Yeh, J. M.; Lin, W. H. Polymer 2003, 44, 2553.
33. Lee, J.; Bhattacharyya, D.; Easteal, A. J.; Metson, J. B. Cur Appl Phys 2008, 8, 42.
34. Rachna, M.; Rao, K. J. Euro Polym J 1999, 35, 1883.
35. Zheng Peng; Ling Xue Kong. Polym Degrad Stab 2007, 92, 1061.
36. Parveen, M. F.; Dhanalakshmi, V.; Anbarasan, R. J Mater Sci 2009, 44, 5852.
37. Anbarasan, R.; Panidarajaguru, R.; Jayalakshmi, T.; Gandhi, S.; Dhanalakshmi, V. J Appl Polym Sci 2010, 117, 2059.
38. Fathima Parveen, M.; Dhanalakshmi, V.; Anbarasan, R. Compos Inter, 2010, 117, 205.